



# Synthesis of adsorbents with dendronic structures for protein hydrophobic interaction chromatography



Marco A. Mata-Gómez<sup>a</sup>, Sena Yaman<sup>b</sup>, Jesus A. Valencia-Gallegos<sup>a</sup>, Canan Tari<sup>c</sup>,  
Marco Rito-Palomares<sup>a,\*</sup>, José González-Valdez<sup>a,\*</sup>

<sup>a</sup> School of Engineering and Sciences, Tecnológico de Monterrey, Ave. Eugenio Garza Sada 2501 Sur, Monterrey, NL 64849, Mexico

<sup>b</sup> Izmir Institute of Technology, Department of Bioengineering, Urla, 35430 Izmir, Turkey

<sup>c</sup> Izmir Institute of Technology, Department of Food Engineering, Urla, 35430 Izmir, Turkey

## ARTICLE INFO

### Article history:

Received 2 February 2016

Received in revised form 16 March 2016

Accepted 20 March 2016

Available online 23 March 2016

### Keywords:

Dendrons

Hydrophobic interaction chromatography

Adsorbent

Resin

## ABSTRACT

Here, we introduced a new technology based on the incorporation of dendrons—branched chemical structures—onto supports for synthesis of HIC adsorbents. In doing so we studied the synthesis and performance of these novel HIC dendron-based adsorbents. The adsorbents were synthesized in a facile two-step reaction. First, Sepharose 4FF (R) was chemically modified with polyester dendrons of different branching degrees *i.e.* third (G3) or fifth (G5) generations. Then, butyl-end valeric acid ligands were coupled to dendrons *via* ester bond formation. UV–vis spectrophotometry and FTIR analyses of the modified resins confirmed the presence of the dendrons and their ligands on them. Inclusion of dendrons allowed the increment of ligand density,  $82.5 \pm 11$  and  $175.6 \pm 5.7$   $\mu\text{mol}$  ligand/mL resin for RG3 and RG5, respectively. Static adsorption capacity of modified resins was found to be  $\sim 60$  mg BSA/mL resin. Interestingly, dynamic binding capacity was higher at high flow rates,  $62.5 \pm 0.8$  and  $58.0 \pm 0.5$  mg/mL for RG3 and RG5, respectively. RG3 was able to separate lipase,  $\beta$ -lactoglobulin and  $\alpha$ -chymotrypsin selectively as well as fractionation of a whole proteome from yeast. This innovative technology will improve the existing HIC resin synthesis methods. It will also allow the reduction of the amount of adsorbent used in a chromatographic procedure and thus permit the use of smaller columns resulting in faster processes. Furthermore, this method could potentially be considered as a green technology since both, dendrons and ligands, are formed by ester bonds that are more biodegradable allowing the disposal of used resin waste in a more ecofriendly manner when compared to other existing resins.

© 2016 Elsevier B.V. All rights reserved.

## 1. Introduction

A major need in the biotech industry is the isolation and purification of proteins from complex mixtures where protein downstream processing may account for up to an 80% of the final product total cost. Hence, the development of novel isolation and purification methodologies or the optimization of the current standardized protocols to achieve the highest purities and yields, raises mayor attention in the design of bioprocesses. In this context, chromatographic methods are the most used techniques for purification of proteins due to the high recovery and purities achieved. Among

these, size exclusion chromatography (SEC), hydrophobic interaction chromatography (HIC), ion-exchange chromatography (IEX), reverse phase chromatography (RPC) and affinity chromatography (AC) are the most common used protein separation chromatographic techniques [1,2].

HIC is a powerful and widely used technique for purification of proteins [3,4]. It is a key methodology when purification of monoclonal antibodies [5–7] is required. It is often used in the final polishing step of downstream processes as it can easily remove high-molecular weight aggregates [8]. HIC relies on the interaction between the hydrophobic regions on the surface of the biomolecules and the ligands on the support under high concentration of salts *i.e.* ammonium sulfate or sodium chloride [3]. There are numerous commercially available adsorbents with different types of hydrophobic ligands *i.e.* butyl, octyl and phenyl groups. However, one of the major drawbacks in HIC is the low ligand density that impacts directly on the adsorption capacity of resins. Furthermore, the methods used to activate the support materials might be

\* Corresponding authors.

E-mail addresses: [matago24@gmail.com](mailto:matago24@gmail.com) (M.A. Mata-Gómez), [senaymn@gmail.com](mailto:senaymn@gmail.com) (S. Yaman), [valencia@itesm.mx](mailto:valencia@itesm.mx) (J.A. Valencia-Gallegos), [canantari@iyte.edu.tr](mailto:canantari@iyte.edu.tr) (C. Tari), [mrito@itesm.mx](mailto:mrito@itesm.mx) (M. Rito-Palomares), [jose\\_gonzalez@itesm.mx](mailto:jose_gonzalez@itesm.mx) (J. González-Valdez).

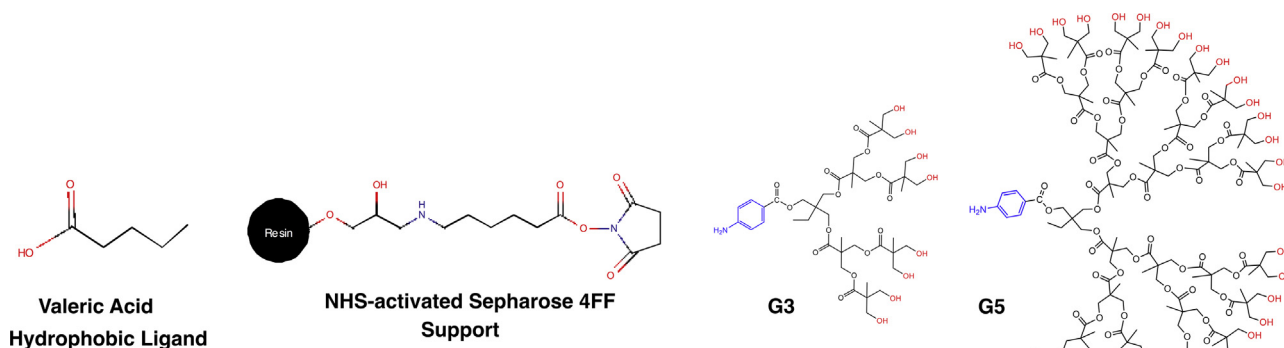


**Fig. 1.** Chemical compounds used for the synthesis of the hydrophobic adsorbents. Chemical structures from left to right are valeric acid, resin, and dendrons of third (G3) and fifth (G5) generations. Marvin was used for drawing, displaying and characterizing chemical structures, substructures and reactions, Marvin 15.8.3.0, 2015, ChemAxon (<http://www.chemaxon.com>).

tedious or are sometimes based on bromide-derived compounds, which are toxic to environment. For this reasons, new HIC matrix functionalization methodologies and options are needed which may also provide further advantages to this commonly used unit operation.

Synthesis of chromatographic media is a challenging task. It requires a precise selection of the chemistry to be used and the reproducibility of the obtained ligand density between batches may become a drawback in this process. Commercially, the most used method for activation of solid supports is achieved through the incorporation of epoxy groups onto the matrix that are subsequently reacted with the desired ligand [9]. This strategy provides a general method to attach ligands for their use in a great variety of separation techniques such as IEX, HIC, RPC or AC and it governs the market. Another method, but not preferable to epoxy activation, is the cyanogen bromide activation method [10]. However, it has major disadvantages such as reagent toxicity, the addition of undesired ion exchange interactions, and the instability of the *N*-substituted isourea linkage that causes improper attachment of the ligands. In contrast, here for the first time, we developed a method for immobilization of ligands based on esterification reactions that yielded stable bonds as resins were reused many times as it will be described later. However, further studies may involve immobilization of ligands based on amide bonds that are even more stable than ester bonds. Nonetheless, the innovation presented here could be considered as a green technology as it is friendly to the environment in terms of waste disposal as ester bonds are more biodegradable than traditional resins based on epoxy reactions.

In this instance, dendrons are a class of synthetic macromolecules that might be tailored for a specific application due to their well-defined structure and flexibility [11]. These polymers possess a branched structure anchored to a focal point of any chemistry, which emanates radially toward the molecular periphery ending in any desired chemical moiety that, in turn, can be functionalized for a specific application [11]. So far, dendritic structures have been widely exploited as nano-carrier systems for drug delivery [12] and in the design of DNA microarrays [13]. There are as well some reports regarding modification of stationary phases with dendrimers [14,15], but not for protein purification.

In this work, we have extended the application of dendritic chemical structures to the synthesis of novel chromatographic adsorbents in an innovative way through their incorporation onto chromatographic matrixes and the subsequent covalent attachment of ligands by formation of ester bonds onto the dendron molecules. The branched architecture of the dendritic molecules allows the attachment of a higher amount of ligands onto the

resin and the generation of hydrophobic clusters throughout it. This results in multiple interaction sites with stronger hydrophobic interactions between the proteins and the adsorbent. This work deals with the synthesis of dendronized adsorbents for protein HIC and their performance in the separation of model proteins and a whole proteome.

## 2. Experimental

### 2.1. Chemicals

Third generation (G3, Cat. No. 767263) and fifth generation (G5, Cat. No. 767239) bis-MPA (2,2-Bis(hydroxyl-methyl) propionic acid) polyester dendrons manufactured by Polymer Factory Sweden AB (Stockholm, Sweden) used for the synthesis of the adsorbents were bought from Sigma-Aldrich (St. Louis, MO, USA). NHS-activated Sepharose 4FF (Cat. No. 17-0906-01) was acquired from GE Healthcare (Uppsala, Sweden). Baker's yeast (*Saccharomyces cerevisiae*) was acquired locally in Monterrey, México. Model proteins including bovine serum albumin (BSA, Cat. No. A4503), lipase (LP, L3126) from porcine pancreas,  $\beta$ -lactoglobulin ( $\beta$ -Lac, Cat. No. L3908) from bovine milk, and bovine pancreatic  $\alpha$ -chymotrypsin ( $\alpha$ -Quym, Cat. No. C4129) were bought from Sigma-Aldrich. *N,N*-dimethylformamide (DMF, Cat. No. 227056), 1-ethyl-3-(3-dimethylaminopropyl) carbodiimide hydrochloride (EDC, Cat. No. E7750), toluene (Cat. No. 244511), ethanol (EtOH, Cat. No. 02860), *N*-hydroxysuccinimide (NHS, Cat. No. 130672), dimethylaminopyridine (DMAP, Cat. No. 107700), valeric acid (VA, Cat. No. 240370), ethyl acetate anhydrous (Cat. No. 270989) and 2-propanol(iso-propOH, Cat. No. 650447) of HPLC grade were also purchased from Sigma-Aldrich (St. Louis, MO, USA). Acetone (Cat. No. AH010) and methanol (MeOH, Cat. No. AH230) of HPLC grade were purchased from Honeywell Burdick and Jackson (Morris Plains, NJ, USA). *p*-Toluensulfonic acid (PTSA, Cat. No. 89762) was bought from Fluka Analytical (St. Louis, MO, USA). All other chemicals used were all at least of analytical grade.

### 2.2. Catalyst synthesis for ester reactions

4-(dimethylamino)pyridinium 4-toluenesulfonate (DPTS) was prepared by reacting equivalent amounts of anhydrous PTSA and DMAP. The latter was dissolved in 40 mL of anhydrous toluene and added to PTSA. The suspension was filtrated, washed with toluene and dehydrated in vacuum. The resulting powder was used in the ester synthesis.

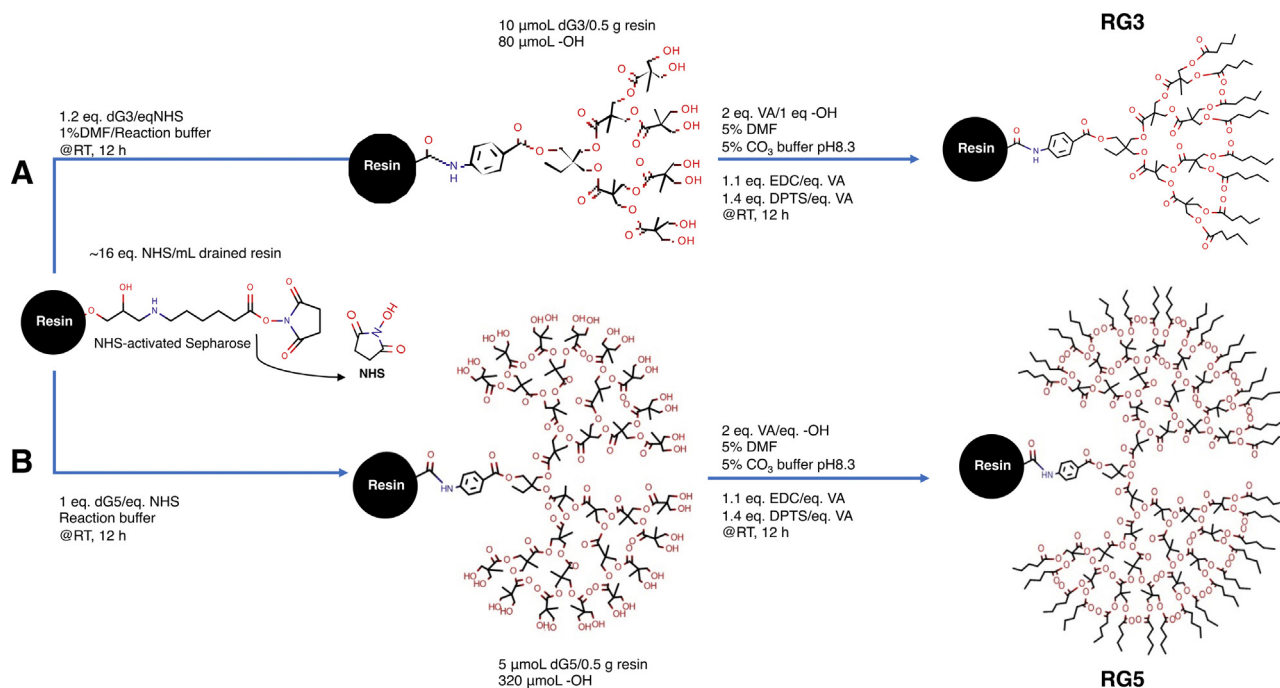


**Fig. 2.** Reaction route for the two-step synthesis of the dendronized adsorbents modified with dendrons (A) G3 and (B) G5. Reactants, conditions, and reaction times are briefly described for each of the steps. Marvin was used for drawing, displaying and characterizing chemical structures, substructures and reactions, Marvin 15.8.3.0, 2015, ChemAxon (<http://www.chemaxon.com>).

### 2.3. Synthesis of dendronized adsorbents

The NHS-activated Sepharose 4FF resin was modified with the G3 and G5 dendrons separately in a two-step strategy. See Fig. 1 for the chemistries used in the synthesis of the HIC adsorbents. In the first step, the dendrons were covalently attached to the resin through the formation of an amide bond and in a second step the free hydroxyl groups present on the dendrons were esterified with valeric acid to activate the support with hydrophobic ligands of 4 carbons. The new adsorbents are referred as RG3 and RG5 along the text. A scheme of the route followed to synthesize the HIC adsorbents is shown in Fig. 2. To synthesize RG3, 4 mL of resin (13–26  $\mu\text{mol}$  NHS/drain mL resin) were first washed with cold 1 M HCl and separated into four 0.5 g batches. Then, 1.2 equivalents of RG3 were dissolved in 0.5 mL of a reaction buffer composed of 100 mM carbonate buffer pH 8.3, 0.5 M NaCl and 1% DMF. The G3 solution was immediately poured into the 2 mL polypropylene screwed cap tubes containing the resin. Reaction was kept in constant agitation for 12 h. After reaction, tubes were centrifuged at 10,000 rpm for 10 min and the supernatant was recovered. The remaining G3 was quantified to estimate the amount of dendron attached to the resin by spectrophotometry as described below. In the second step, the RG3 resin (10  $\mu\text{mol}$  G3/0.5 g wet resin) containing  $\sim 80$  equivalents of hydroxyl groups per  $\mu\text{mol}$  of G3 was then functionalized with valeric acid. To do this, RG3 was first dehydrated with acetone:H<sub>2</sub>O solutions (1:2, 1:1 and 3:1, consecutively) and pure acetone. After this, the resin was washed twice with DMF and the excess of solvent was removed by filtering it through a sintered glass funnel. Two grams of the resin were divided into four batches. Two equivalents (160  $\mu\text{mol}$ ) of valeric acid with respect to the amount of  $-\text{OH}$  groups in the dendron were dissolved in 1 mL of a solution of DMF/5% carbonate buffer at pH 8.3. To this mixture, according to the amount of valeric acid, 10% and 40% excess of EDC and DPTS, respectively, were added. The mixture was then kept in constant agitation at room temperature during 12 h.

The RG5 was synthesized following the same protocol described for the RG3 adsorbent. The only difference was that the reaction buffer for the first step did not required addition of DMF. The obtained resin modified with G5 (5  $\mu\text{mol}$  G5/0.5 g wet resin), with  $\sim 32$  equivalents of hydroxyl groups/ $\mu\text{mol}$  G5, was butylated as described above. In this case, two equivalents (320  $\mu\text{mol}$ ) of valeric acid with respect to the amount of  $-\text{OH}$  groups in the dendron, were dissolved in the same solvent system used in the previously described step and the reaction was conducted in the same way.

After the reactions were completed, all of the obtained modified adsorbents were washed with DMF, acetone:H<sub>2</sub>O solutions, but this time in reverse order starting with pure acetone. Finally, the adsorbent was washed with 20% EtOH and stored at 4 °C for subsequent experiments.

### 2.4. Analytical estimations

The G3 and G5 dendrons were quantified by UV spectrophotometry. For this, UV–vis spectra of both dendrons and the  $-\text{NHS}$  group, which leaves the resin during reaction, were first recorded in order to determine their maximal absorption wavelengths. Note that the leaving group  $-\text{NHS}$  in the resin absorbs at 215 nm, thus to eliminate its interference, calibration curves of either dendron or NHS were obtained at both maximal absorption values. Dendron concentration was calculated by solving a simple linear equation system taking into account the extinction molar coefficients of the dendrons and NHS as well as the absorbance measurements recorded. Absorbance measurements of 100  $\mu\text{L}$  samples were recorded in a microplate reader (Epoch Microplate Reader; Biotek, VY, USA). All estimations were performed by triplicate.

Estimation of valeric acid attached to resin was performed by HPLC (Varian) equipped with a Luna 5  $\mu\text{m}$  C18 column of 100 Å and 150  $\times$  4.6 mm (Phenomenex, CA, USA). The mobile phase used was 60% methanol:40% H<sub>2</sub>O at pH 2.3.

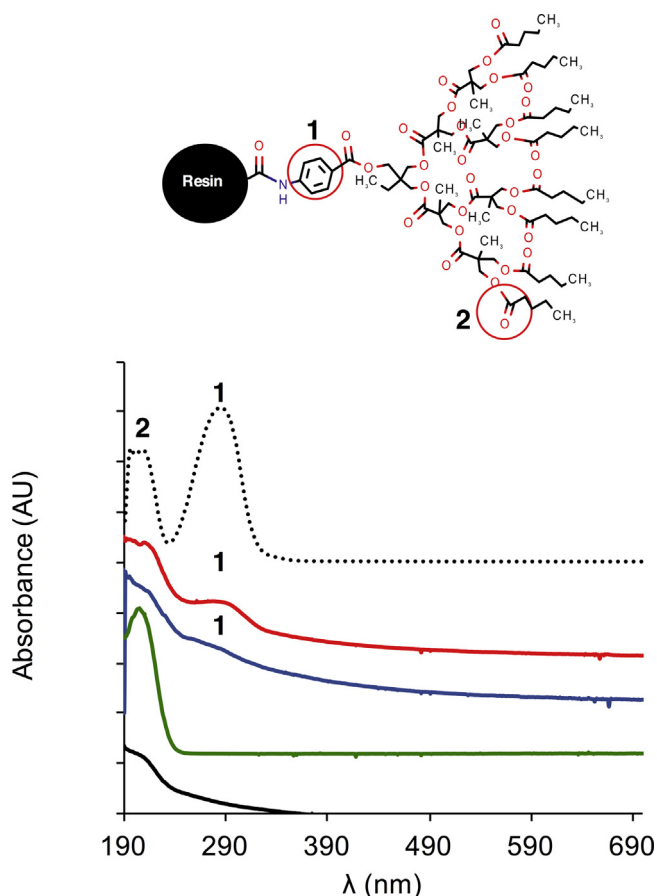


**Fig. 3.** Comparison of UV–vis spectra of various resins. Black line: unmodified resin, red line: RG3, blue line: RG5, dotted black line: pure G5, green line: valeric acid. Numbers 1 and 2 correspond to benzyl and carbonyl groups, respectively, as depicted in the structure on the top of the figure. Graphed values are the mean of three replicates. Marvin was used for drawing, displaying and characterizing chemical structures, substructures and reactions, Marvin v15.8.3.0, 2015, ChemAxon (<http://www.chemaxon.com>). (For interpretation of the references to color in this figure legend, the reader is referred to the web version of this article.)

### 2.5. Chemical characterization of the novel dendron-based adsorbents

Dendronized adsorbents were characterized by UV–vis spectrophotometry and FTIR analysis. UV–vis absorption spectra were recorded with a Genesys 10S UV–vis spectrophotometer (ThermoFisher Scientific, MA, USA). For this, 100 mg (wet basis) of unmodified or dendronized resin were suspended in 1 mL of distilled water and transferred into a 1 cm path length quartz cuvette. Scanning of samples was performed in a wavelength range of 190–700 nm. Infrared analysis was performed in an FT-IR/FT-NIR spectrometer (Spectrum 400; PerkinElmer, MA, USA) in the range of 400–3500  $\text{cm}^{-1}$ . All experiments were performed by triplicate.

### 2.6. Adsorption experiments

Adsorption experiments of the dendronized adsorbents were performed either in static or dynamic mode using bovine serum albumin (BSA) as model protein. For experiments in static mode (SAC), adsorption was carried out in batches. To do this, 100 mg of resin, on wet basis (*i.e.* RG3 or RG5), were transferred into 2-mL screw-capped microtubes and equilibrated with 1.5 or 2 M ammonium sulfate (AS). Then resin was filtered with a sintered glass funnel and two-mL solutions of BSA (0–3 mg/mL) prepared in 1.5 or 2 M AS were mixed with the resin. Adsorption was conducted

for 15 min under constant stirring using a revolver mixing system. Resin was separated from the solution by centrifugation. The unabsorbed protein (concentration in the equilibrium) was measured in the supernatant with a microplate assay based on the Bradford method [16]. Assays were carried out in triplicates. The bound amount of protein ( $q$ ) in mg/mL wet resin was calculated by mass balance according to the following equation:

$$q = \frac{(c_0 - c)V}{V_R} \quad (1)$$

In the above equation  $c_0$  and  $c$  represent the initial protein concentration and the protein concentration at the equilibrium, respectively, in mg/mL,  $V$  is the volume of the solution, and  $V_R$  stands for the volume of the adsorbent in mL. Unmodified resin was used as control. Experimental data were fitted to a Langmuir mathematical model by using a non-linear regression model with the following equation:

$$q = \frac{q_m C_e}{K_d + C_e}, \quad (2)$$

where  $q$  is the amount of protein bound to the adsorbent in mg/mL wet resin,  $q_m$  stands for the adsorption capacity in the equilibrium in mg/mL wet resin,  $C_e$  is the concentration of protein in the equilibrium in mg/mL, and  $K_d$  denotes the affinity constant in mg/mL.

Saturation curves for dynamic binding capacity (DBC) were obtained with a 1-mL Tricorn™ 5/50 column packed with either the HIC RG3 or RG5 adsorbents. The column was connected to an Äkta pure chromatography system (GE Healthcare, Uppsala, Sweden) and equilibrated with buffer A composed of 20 mM Tris-HCl at pH 7 containing 1.5 or 2 M AS salt. Protein solutions of 40 mL (1–3 mg BSA/mL) were injected into the column using a 50-mL superloop (GE Healthcare, Uppsala, Sweden). Experiments were ran at two different flow rates (1 and 2 mL/min) and two concentrations of AS (1.5 and 2 M). Chromatographic runs comprised of six steps including equilibration (5 mL), injection (40 mL), washing (10 mL), elution (5 mL), a second wash (10 mL) and another final equilibration step (5 mL). After saturating the column, protein adsorbed was eluted by pumping buffer B (20 mM Tris-HCl at pH 7) without salt into the column in one step. To calculate protein concentration, each point of the curve was integrated by obtaining delta volumes (mL) of two consecutive points in axis  $x$  and multiplying by the height (mAU) of each point. These areas were then compared to the total area under the curve (mAU\*mL), considered as the total start proteic material loaded onto the column in order to estimate mass (mg). Finally, the mass was divided by the corresponding delta volume to calculate protein in mg/mL. DBC at 10% breakthrough (DBC<sub>10%</sub>) was calculated using the following expression:

$$DBC_{10\%} = \frac{c_0(V_{10\%} - V_0)F}{V_B} \quad (3)$$

where  $c_0$  is the fed concentration of protein in mg/mL,  $V_{10\%}$  is the volume in mL applied at 10% breakthrough,  $V_0$  is the void volume in mL of the column,  $F$  is the flow rate in mL/min, and  $V_B$  is the volume (mL) of the bed. All of the experiments were performed in triplicate.

### 2.7. Dendron-based HIC with model proteins

Performance of the RG3 adsorbent was tested with various pure protein models, which were: lipase (LP),  $\beta$ -lactoglobulin ( $\beta$ -Lac) and  $\alpha$ -chymotrypsin ( $\alpha$ -Chym). HIC experiments were performed in the same chromatographic system described above using a 1-mL column packed with RG3, which was equilibrated with buffer A containing 1.75 M of AS. Samples of the proteins by separate or a mixture of the three proteins were dissolved in buffer A and loaded onto the column using a 0.1 mL loop. Elution was done by applying



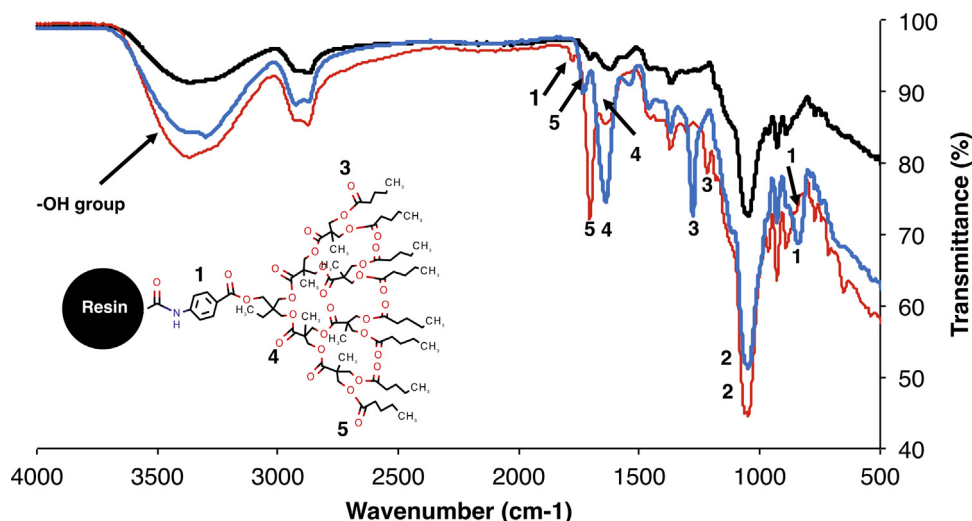


**Fig. 4.** Comparison and FTIR analysis of the adsorbents. Black line: unmodified resin, red line: RG3, blue line: RG5. Numbers depicted in both the inset chemical structure in the graph and the various peaks are 1: Benzyl, 2: glycosidic bond in agarose, 3: ester bond, 4: interior carbonyl group, 5: exterior carbonyl group. Marvin was used for drawing, displaying and characterizing chemical structures, substructures and reactions, Marvin 15.8.3.0, 2015, ChemAxon (<http://www.chemaxon.com>). (For interpretation of the references to color in this figure legend, the reader is referred to the web version of this article.)

a five-step gradient at a flow rate of 1.5 mL/min. Concentration of salt started at 1.75 M and decreased in each step to 1.4, 1.05, 0.7 and 0.35 M until 0% of AS was reached. The length of each step was of 10 mL. Three independent runs were performed.

### 2.8. Whole proteome processing in dendron-based adsorbents

Proteome from *Saccharomyces cerevisiae* was fractionated with the RG3 adsorbent. Commercial yeast was washed overnight with distilled water and centrifuged at 10,000 rpm and supernatant was discarded. Biomass (15 g) was suspended in 15 mL buffer Tris-HCl 20 mM at pH 7 and lysate using a 20 kHz sonicator (QSonica, model Q125, Newtown, CT, USA) equipped with a CL-18 probe. The sonicator was operated at an amplitude of 60% in 20 s pulses on with intervals of 10 s pulses off during 15 min. Suspension was centrifuged at 10,000 rpm and supernatant (10 mL) was concentrated using 5 mL-Amicon units (Merck Millipore). Two lots of concentrated supernatant (2.5 mL) were desalted on PD10 columns (GE Healthcare). After desalting the sample for several times, the protein solution was concentrated up to 10 mL and AS (1.75 M) was added. A micro-filtered sample of 5 mL was injected onto the column packed with RG3 in the same chromatographic system described above through a 5-mL loop. The elution was performed in the same way as it was done for pure proteins, but this time a 1 mL/min flow rate was applied. Experiments were conducted by triplicate. Fractions of 2 mL were collected, concentrated and analyzed by SDS-PAGE [17]. For this, protein samples were routinely prepared by mixing them with 6X Laemmli sample buffer, containing 27 mM dithiothreitol, in a 5:1 proportion and heating at 95 °C during 5 min. Then samples (10–15  $\mu$ L) were loaded into a 4–20% precast polyacrylamide gel (BioRad, Cat. No. 4561094) and resolved at 150 V (25 mA) for 35 min in a Mini-PROTEAN® Tetra Cell (BioRad). Protein bands were visualized using colloidal Coomassie G-250 staining [18].

## 3. Results and discussion

### 3.1. UV-vis absorption spectra of the novel adsorbents

UV-vis spectra of the unmodified and dendronized resins are presented in Fig. 3. The unmodified resin exhibited a maximum absorption band at  $\sim$ 212 nm that can be attributed to carbonyl

groups present in the NHS group. In the case of the RG3 and RG5 adsorbents, both exhibited two bands at 206 and 290 nm, which are more visible in RG3. In the modified resins, the appearance of the maximum absorption bands at  $\sim$ 290 nm, that coincide with those bands of the pure G3 and G5 dendrons, indicates the insertion of the dendron since this absorption is typical of the phenyl ring, which is present in both dendrons. The absence of bands in the unmodified resin around 290 nm confirms that the resin was indeed modified with the dendrons. It should be mentioned however that ester groups (transition  $n-\pi^*$ , C=O) may absorb around  $\sim$ 273 nm, which may overlap with the absorption band of the phenyl group at  $\sim$ 290 nm. This may explain the broadened absorption bands for both RG3 and RG5 as compared to unmodified resins. Note that the G5 dendron has more ester groups, which could explain the fact that the  $\sim$ 290 band of RG5 is not as well defined as it is in RG3. The two modified resins showed absorption bands around 208 nm, which are consistent with the carbonyl group absorption spectra of valeric acid as well as with that band of the pure G5 at the same wavelength. This may indicate the presence of valeric acid esterified onto the resin as well as the presence of the ester carbonyl groups abundant in the dendrons.

### 3.2. Reaction verification by infrared analysis

The infrared spectra of the adsorbents synthesized are presented in Fig. 4. The characteristic peak at  $1050\text{ cm}^{-1}$  corresponding to the glycosidic bond of agarose shown in the unmodified resin and observed in the dendronized adsorbents suggests that the method here presented maintains the chemical structure of the agarose matrix untouched. It should be mentioned that the symmetric stretch of ester R–O–COR also absorbs at  $\sim$ 1050  $\text{cm}^{-1}$ ; however, the corresponding band may overlap with the very intense absorption band of the glycosidic bond (entry 2 in Fig. 4). The presence of both dendron molecules attached onto the support are revealed by the appearance of a peak around 800–840  $\text{cm}^{-1}$ , which is smaller for RG3, and corresponds to the phenyl ring; this signal is not present in the unmodified resin confirming that the dendron is attached. Besides, this signal indicates a *para* substitution that suggests that from one side of the phenyl ring the dendron molecule is attached to the resin and from the other side the first block of the dendron is maintained. In the case of the adsorbent modified with G3, the presence of an overtone peak at  $1748\text{ cm}^{-1}$  also

**Table 1**  
Infrared peak assignment for the dendronized adsorbents.

No. Peak	Peak assignment	Frequency (cm <sup>-1</sup> )		
		Unmodified	RG3	RG5
1	Benzyl	–	838, 1748	838–840
2	Glycosidic —O—	1050	1050	1050
3	Ester R—O—COR	–	1218	1280
4	<sup>a</sup> Carbonyl C=O	1587	1635	1636
5	<sup>b</sup> Carbonyl C=O	1700	1704	1730
6	—OH	3300	3300	3300

<sup>a</sup> Internal carbonyl groups in the dendrons.

<sup>b</sup> External carbonyl groups in the dendrons.

suggests the incorporation of the dendron, as this signal is typical for benzyl rings. The signals at 1218 and 1280 cm<sup>-1</sup> exhibited by RG3 and RG5, respectively, not present in the unmodified resin, correspond to typical stretching of ester groups present in the dendronized adsorbents. The peaks at around 1635 cm<sup>-1</sup> (peak No. 4) indicate the presence of internal carbonyl groups corresponding to esters groups in both dendron structures, while the signals at 1704 and 1730 cm<sup>-1</sup> correspond to the periphery carbonyl groups of the valeric acid attached to the RG3 and RG5, respectively. A summary of the peak assignment is listed in Table 1.

### 3.3. Chemical synthesis of dendron-based adsorbents

We have introduced a simple method to synthesize two adsorbents based on dendronic structures for HIC of proteins. The synthesis is reached in a two-step method that includes the incorporation of the dendron and the immobilization of the ligands (see Fig. 2). The matrixes were first chemically synthesized by covalently attaching the amine core of bis-MPA polyester dendrons of two generations, third (G3) and fifth (G5) generations to NHS-activated Sepharose 4FF chromatographic resin under alkali conditions. The dendronized resins were then functionalized through organic carboxylic acid incorporation via an esterification reaction with the available hydroxyl groups (—OH) on the dendrons in aqueous-organic media. This leaved clusters of butyl groups on the periphery of the dendron molecules free to act as hydrophobic ligands. Note that we started with the incorporation of a five-carbon carboxylic acid (*i.e.* valeric acid) to create butyl ligands, but this strategy can be potentially extended to the incorporation of any ligand containing a carboxyl group to create adsorbents with different hydrophobic natures or even activate adsorbents for other protein purification applications such as IEX, RPC and AC.

Table 2 presents the dendron and ligand density on the support achieved with this technology. As hypothesized, the structural nature of these dendrons allowed enhancing the amount of ligands on the surface of the support. Note that the ligand density depends directly on the number of branches. As noticed, it was possible to incorporate a larger amount of G3 dendron (10 μmol/mL resin) to the adsorbent as compared to G5. The fact that a smaller amount G5 is attached onto the resin is due to steric effects as G5 is ~4 times bigger than G3, making it more difficult for G5 to react properly. It is important to mention that despite the amounts of dendrons grafted to the matrix the procedure allowed the incorporation of a higher amount of ligands as compared to commercial HIC resins, whose ligand densities vary between 9 and 53 μmol ligand/mL resin, depending on the type of ligand (butyl or phenyl). These HIC media exhibit a dynamic capacity ranging between 31 and 40 mg BSA/mL medium as determined by their fabricant, GE healthcare. Thus, this technology may solve the drawbacks related to low ligand density when developing new HIC adsorbents. Nonetheless, it is necessary to optimize the process to control the ligand density among batches and to maximize it as much as possible. As the

ligand density is related to the adsorption capacity of the resin, the higher the ligand density, the higher the adsorption capacity. Therefore, it will be possible to use lower amounts of resin to adsorb higher amounts of protein or other molecules of interest. This would also allow the use of smaller columns speeding the complete chromatographic processes. To the best of our knowledge, this is the first work describing the activation of solid supports with dendritic molecules to serve as chromatographic adsorbents for the downstream processing of proteins via HIC.

### 3.4. Static and dynamic adsorption capacities

Adsorption capacity performance for the synthesized resins was evaluated in static and dynamic modes. Experimental data was fitted into Langmuir models. Adsorption isotherms, obtained from static experiments, for both adsorbents RG3 and RG5 are presented in Fig. 5. Experimental points fitted properly in the curve that was simulated according to the Langmuir model. As expected, the capacity of the two resins to adsorb protein was superior at high concentrations of salt (2 M). Both adsorbents showed a similar adsorption capacity, 52 and 59 mg BSA/mL wet resin for RG3 and RG5, respectively. Although both resins have similar adsorptions, it has to be noted that RG3 exhibited a higher affinity, as the  $K_d$  value of  $0.2 \pm 0.01$  mg/mL obtained was lower when compared to that of the RG5 of  $0.5 \pm 0.03$  mg/mL at high concentrations of salt (2 M). In this sense, it was expected that the resin modified with the G5 dendron would show a higher adsorption and a major affinity, as it has more —OH groups, sites where ligands can be attached. The facts that both resins exhibited similar adsorption capacities and that RG3 has a major affinity can be explained in terms of dendron or ligand densities. RG3 on its part, has a major density of dendron molecules attached to the matrix in comparison to RG5, thus there are more hydrophobic cluster sites to interact when protein molecules travel along with the fluid; this also explains the higher affinity exhibited by RG3 toward proteins. On the other hand, although RG5 has a lower amount of dendrons than RG3, it does have a higher ligand density (see Table 1), and therefore the adsorption capacity may be compensated. In other words, RG5 needs half the amount of dendron molecules per mL of wet resin to adsorb the same amount of protein as RG3 does (Table 3).

In addition, other parameters different than ligand density could also influence the adsorption capacity of the resins *i.e.* the size of the ligand and the interaction between ligands and protein molecules. In the first case, butylated-dendron ligands are much higher in surface than butyl ligands, therefore dendrons may rise some steric effects that somehow could affect adsorption capacity. Even more, interaction of protein molecules with the butylated branched dendrons disposed in the surface of the resin beads, more specifically in the mouth of the outer pores of the resin beads, may reduce the pore size by clogging and therefore limiting the mass transfer to the interior pores; this naturally will impact the adsorption capacity as demonstrated before for other ligands in ion exchange chro-

**Table 2**  
Dendron and ligand densities on the surface of the synthesized adsorbents.

Adsorbent	Dendron	Dendron MW (Da)	Batch	$\mu\text{mol dendron/mL resin}$	$\mu\text{mol ligand/ml resin}$
RG3	G3	950	1–4	<sup>a</sup> 10.1 ± 0.5	<sup>a</sup> 82.5 ± 4.2
				<sup>b</sup> 9.0, 9.7, 10.0, 11.5	<sup>b</sup> 71.2, 81.1, 88.5, 89.3
RG5	G5	3722.7	1–4	<sup>a</sup> 5.6 ± 0.3	<sup>a</sup> 175.6 ± 5.6
				<sup>b</sup> 5.2, 6.5, 59.4, 9	<sup>b</sup> 162.0, 182.8, 186.5, 170.9

<sup>a</sup> Data represents the mean of four batches with their standard error.

<sup>b</sup> Data batch-to-batch repeatability.

**Table 3**  
Adsorption capacity of the dendronized resins in static mode.

Adsorbent	Parameter [Ammonium sulfate, M]	Batch	$q$ (mg/mL wet resin)		$K_d$ (mg/mL)	
			1.5	2	1.5	2
RG3	1.5	1–4	<sup>a</sup> 21.3 ± 1.5	<sup>a</sup> 52.4 ± 3.4	0.3 ± 0.03	0.2 ± 0.01
			<sup>b</sup> 18.0, 20.3, 22.0, 25.0	<sup>b</sup> 54.5, 48.4, 60.9, 45.6		
RG5	2	1–4	<sup>a</sup> 21.0 ± 1.1	<sup>a</sup> 58.2 ± 2.5	1.8 ± 0.06	0.5 ± 0.03
			<sup>b</sup> 19.3, 23.5, 19.2, 22.1	<sup>b</sup> 63.1, 58.3, 51.2, 60.1		

<sup>a</sup> Data represents the mean of four batches with their standard error.

<sup>b</sup> Data batch-to batch repeatability.

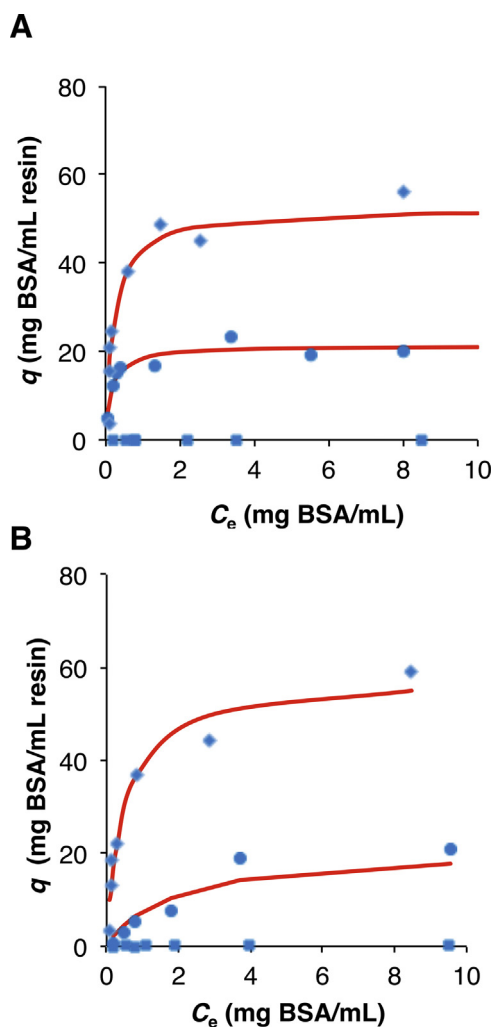


**Fig. 5.** Adsorption capacities of (A) RG3 and (B) RG5 in static mode. Squares correspond to unmodified resin at 2 M ammonium sulfate. Circles and diamonds are 1.5 M and 2 M ammonium sulfate concentrations, respectively. Red lines represent the Langmuir models obtained as described in the experimental section. Values are the mean of three replicates. (For interpretation of the references to color in this figure legend, the reader is referred to the web version of this article.)

matographic methods [19]. Besides, the fact that there are many sites in the surface of the matrix does not guarantee that all of the ligand molecules are occupied by protein molecules; the shielded ligand molecules, as a consequence of its interaction with protein molecules, may impede other protein molecules from interacting with the ligands.

In this same line, another important test to characterize chromatographic resins is to show their capacity to adsorb molecules under a dynamic process as they are commonly used in practical applications. Here we evaluated the dynamic binding capacity of both adsorbents under various conditions including salt and feed protein concentrations, and flow velocity. Breakthrough curves of BSA are presented in Fig. 6. As expected, all the factors tested influenced the shape of the curves. In all cases, it was observed that at high salt concentrations (2 M), the curves presented a higher tilt indicating that a higher amount of protein is adsorbed under these conditions. In contrast, it can be noticed that a plateau-like curve is reached in lower times at lower salt concentrations (1.5 M) resulting in a lower amount of adsorbed protein. At the plateau, the amount of feed protein equals the amount of protein in the outlet of the column. Thus the faster the plateau is reached, the faster the adsorbent saturates. At lower salt concentrations, hydrophobic ligands may not be exposed, thus it becomes less probable for protein molecules to interact with the ligands. Therefore the adsorbent saturates more rapidly. Note that the curves of RG5 obtained at 1 mL/min seem to have a steeper slope indicating that this adsorbent saturates faster than RG3. This is also explained in relation to the lower dendron density in the G5 modified resin as compared to RG3 where there are not as many interactions sites.

The effect of protein concentration on adsorbent saturation is also clearly observed in both resins. The higher the protein concentration, the faster the adsorbents saturated regardless of the salt concentration. In other words, at high protein concentrations, interaction of BSA molecules with ligands is faster occasioning saturation in less time. Notice that at a high flow rate (*i.e.* 2 mL/min), the increasing concentration of protein is faster than at 1 mL/min. Furthermore, it is been observed that at low protein concentration, absorption occurs only in the outer region of the resin particles [20].

The DBC values listed in Table 4 were calculated from each one of the breakthrough curves shown in Fig. 6. The higher the salt concentration, the higher the DBC was. A similar tendency was observed as the protein concentration increased. The highest DBC was exhibited at high flow rates (2 mL/min), 62.5 ± 0.8 and 58.0 ± 0.5 mg BSA/mL for RG3 and RG5, respectively. Commercial butylated chromato-

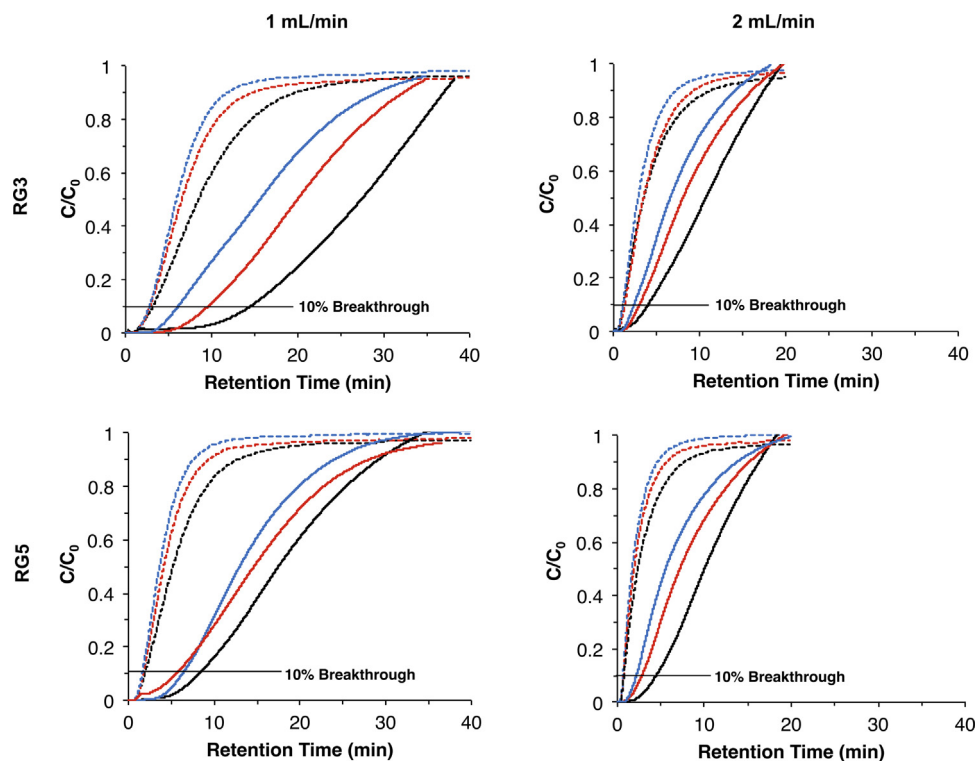


**Fig. 6.** Breakthrough curves of BSA in dendronized adsorbents. The two ammonium sulfate concentrations used were 1.5 M and 2 M that are represented by dashed lines and solid lines, respectively. The colors of the lines indicate the various concentrations of BSA used (black lines, 1 mg/mL; red lines, 2 mg/mL; and blue lines, 3 mg/mL). Each column of graphs corresponds to each of the two flow rates used (1 and 2 mL/min). All presented values are the mean of three replicates. (For interpretation of the references to color in this figure legend, the reader is referred to the web version of this article.)

**Table 4**  
Dynamic binding capacity of dendronized resins.

Adsorbent	Flow rate (mL/min) BSA (mg/mL)	Run	DBC <sub>10%</sub> (mg BSA/mL wet resin)			
			1		2	
			Ammonium sulfate (M)		Ammonium sulfate (M)	
			1.5	2	1.5	2
RG3	1	1–3	<sup>a</sup> 6.3 ± 0.6	<sup>a</sup> 32.2 ± 0.2	<sup>a</sup> 9.0 ± 0.1	<sup>a</sup> 36.0 ± 0.47
			<sup>b</sup> 5.4, 9.2, 6.3	<sup>b</sup> 32.0, 32.6, 28.4	<sup>b</sup> 8.8, 9.2, 9.0	<sup>b</sup> 36.5, 36.2, 35
	2	1–3	<sup>a</sup> 11.5 ± 0.35	<sup>a</sup> 42.5 ± 0.7	<sup>a</sup> 21.0 ± 0.40	<sup>a</sup> 53.4 ± 0.6
			<sup>b</sup> 10.9, 11.5, 12.1	<sup>b</sup> 43.0, 43.3, 41.2	<sup>b</sup> 21.6, 20.3, 21.1	<sup>b</sup> 54.5, 53.5, 52.2
	3	1–3	<sup>a</sup> 17.2 ± 0.01	<sup>a</sup> 42.4 ± 0.1	<sup>a</sup> 25.7 ± 0.51	<sup>a</sup> 62.5 ± 0.8
			<sup>b</sup> 17.1, 17.2, 17.2	<sup>b</sup> 40.2, 42.0, 45.1	<sup>b</sup> 26.4, 25.9, 24.7	<sup>b</sup> 63.5, 62.9, 61
RG5	1	1–3	<sup>a</sup> 4.0 ± 0.03	<sup>a</sup> 12.4 ± 0.2	<sup>a</sup> 6.5 ± 0.3	<sup>a</sup> 40.0 ± 0.2
			<sup>b</sup> 4.0, 4.0, 4.1	<sup>b</sup> 12.3, 12.8, 12	<sup>b</sup> 6.0, 6.4, 7.0	<sup>b</sup> 40.5, 40.5, 41.0
	2	1–3	<sup>a</sup> 7.2 ± 0.006	<sup>a</sup> 37.1 ± 0.08	<sup>a</sup> 11.4 ± 0.2	<sup>a</sup> 47.5 ± 2.17
			<sup>b</sup> 7.3, 7.3, 7.2	<sup>b</sup> 37, 37.3, 37	<sup>b</sup> 11.6, 11.7, 11.0	<sup>b</sup> 43.1, 49.7, 49.5
	3	1–3	<sup>a</sup> 9.6 ± 0.3	<sup>a</sup> 42.0 ± 0.5	<sup>a</sup> 15.8 ± 0.1	<sup>a</sup> 58.0 ± 0.5
			<sup>b</sup> 9.7, 10.1, 9.0	<sup>b</sup> 42.1, 42.8, 41	<sup>b</sup> 15.8, 15.7, 16	<sup>b</sup> 58.5, 58.5, 57.6

<sup>a</sup> Values were obtained at 10% breakthrough. Data represents the mean of three runs with their standard error.

<sup>b</sup> Data run-to-run repeatability.

graphic adsorbents offer adsorption capacities varying from 27 to 39 mg BSA/mL medium, as obtained from GE Healthcare data sheet products, under dynamic conditions. Normally, lower residence times decrease the DBC [21], while longer residence times lead to higher adsorption capacities as the protein molecules have more time to travel to interior of the pores of the resin beads and interact to a great extent with ligands [22]. Interestingly, in this work the DBC was higher as the flow rate increased. In this tenor, it should be noted that new synthetic adsorbent materials have been recently introduced to the market by YMC Separation Technology with high DBCs even at higher linear velocities [23]. In our case, the observed high DBC at the tested linear flows could be explained by two hypotheses. The first one is that due to their nature, dendrons

allow the attachment of a higher amount of ligands forming clusters that increase the probability for protein molecules to interact as they are passing through the interstitial spaces of the resin. The second one is that dendronic structures in G3 and G5 are much larger than butyl ligands and therefore during the synthesis reaction dendrons are more likely to be attached to the outer surface of the resin beads and therefore protein molecules do not necessarily travel to the interior of the beads to be adsorbed. It should be remarked however, that the presented DBCs at high flow rates could potentially speed the chromatographic processes saving time, reagents and increasing the capacity of the whole operation as more sample can be processed in each chromatographic run.



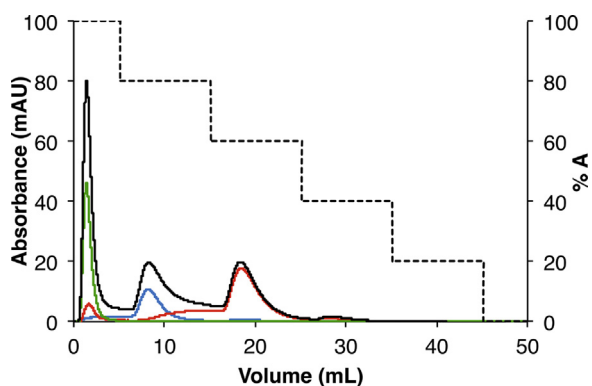


**Fig. 7.** Separation of model proteins using the dendronized RG3 adsorbent. Each of the tested protein samples are depicted as follows: green chromatogram: lipase (4 mg/mL), blue chromatogram:  $\beta$ -Lactoglobulin (3 mg/mL), red chromatogram:  $\alpha$ -Chymotrypsin (3.5 mg/mL) and black chromatogram: mixture of the three model proteins at the same concentrations mentioned. The dotted line represents the decreasing step gradient of salt. Flow rate was 1.5 mL/min. The volume length for each step was of ten mL. Starting buffer is composed of 20 mM Tris-HCl pH7/1.75 M ammonium sulfate. Retention volumes (mL) for model proteins are: lipase: 1.41, 1.39, and 1.45;  $\beta$ -Lactoglobulin: 8.18, 8.20 and 8.15;  $\alpha$ -Chymotrypsin: 18.43, 18.41, 18.39. The presented chromatograms are the mean of three replicates. (For interpretation of the references to color in this figure legend, the reader is referred to the web version of this article.)

### 3.5. Chromatographic performance of the synthesized adsorbents

For these experiments, the RG3 adsorbent was selected since it has a higher ligand density as previously mentioned. The separation of pure proteins was first attempted and Fig. 7 presents the separation of three model proteins with RG3. From the three proteins, LP was not adsorbed onto the resin and was eluted into the flow through, while  $\beta$ -Lac and  $\alpha$ -Chym were adsorbed and were subsequently eluted when the concentration of salt decreased from 1.75 M (100%) to 1.4 M and 1.05 M, respectively. This evidenced that the three proteins have different affinities for the adsorbent and can therefore be resolved. Notice that retention times of individual proteins match with the three peaks observed in the profile of the mixture of proteins confirming that proteins were separated selectively.

In a second experiment, RG3 was tested to fractionate a more complex sample such as a whole proteome. Fig. 8 presents a chromatogram of the fractionation of the proteome from *S. cerevisiae*. As seen, five peaks were obtained. The flow-through peak includes all the proteins that were not adsorbed into the resin and were washed out from the column during the washing step, previous to the beginning of the elution step. The other four peaks (I–IV) correspond to proteins that were adsorbed onto the resin and subsequently desorbed selectively by reducing the concentration of salt in various steps. Additionally, the SDS-PAGE gel in Fig. 8 shows the different protein profiles obtained in each fraction in comparison to that of the whole proteome. As expected, the profile of proteins in each fraction is different suggesting that the proteins from the proteome from *S. cerevisiae* present different hydrophobicity and therefore can be separated according to this property. It should be noted that HIC fractionation of a yeast proteome using various commercial adsorbents with ligands with different hydrophobicity strength exhibited similar results as compared to RG3 [3]. Even more, with these results the practical capability of these novel dendron-based adsorbents is shown giving step to their incorporation in different processes once optimization of both synthesis and operation is achieved.

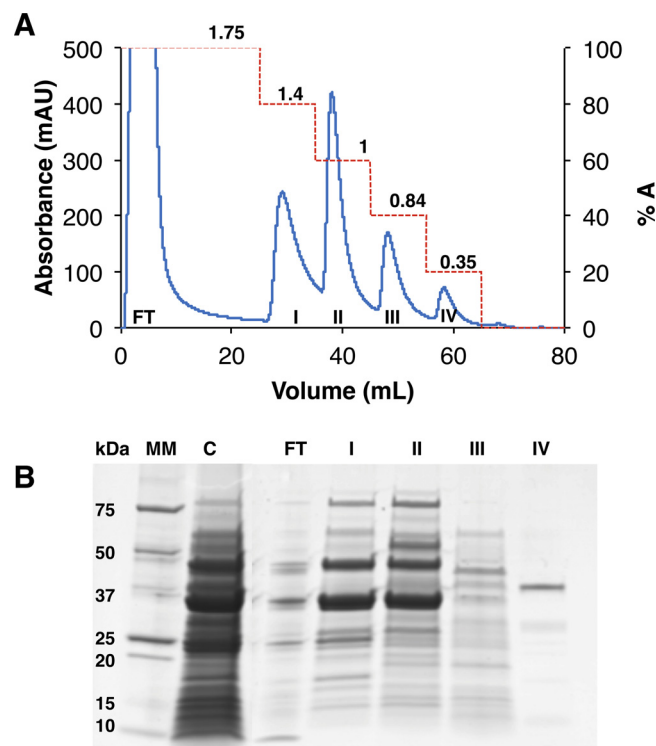


**Fig. 8.** (A) Fractionation of a whole proteome from *Saccharomyces cerevisiae* with RG3 and (B) SDS-PAGE image of the obtained fractions. In (A) and (B): FT corresponds to the flow through and roman numerals represent the obtained fractions from I–IV. In (B) MM and C denote the molecular weight marker and the crude extract, respectively. The dotted red line is the decreasing step gradient of salt and the ammonium sulfate concentrations in molar (M) units are indicated in each step. Flow rate was maintained at 1 mL/min. The volume length for each step was of ten mL. The starting buffer was composed of 20 mM Tris-HCl pH7/1.75 M ammonium sulfate. The values presented are the mean of three replicates. (For interpretation of the references to color in this figure legend, the reader is referred to the web version of this article.)

## 4. Conclusions

A new technology to modify and activate supports through the incorporation of dendronic structures onto the chromatographic matrix has been developed. This was achieved by subsequently immobilizing ligands *via* ester bond formation between hydroxyl groups of dendrons and the carboxylic groups of the valeric acid, the latter being the ligand. The synthesis is reached in a simple two-step method. One advantage of this technology is that as the ligand density is related to the adsorption capacity of the resin, the higher the ligand density is, the higher the adsorption capacity will be. Other parameters such as the ligand size should also be considered when synthesizing resins of such a nature as ligands large in surface may reduce effective pore size impeding protein molecules from being adsorbed, which could lead to reduced adsorption capacities. Other ligands with less size but containing more hydroxyl groups could improve the steric effects problems which difficult mass transfer. With this technology it is possible to use lower amounts of resin to adsorb higher amounts of protein or other molecules of interest. This also allows the use of smaller columns and thereby the acceleration of the chromatographic processes. Even more, the high dynamic capacity observed at high flow rates will accelerate the process while increasing the capacity to process larger sample amounts in less time.

This strategy based on dendronic structures seems to be a promising technology, not only to solve the problems related to low ligand densities in commercial HIC adsorbents, but also to increase the ligand density on other types of chromatographic techniques like IEXC and affinity chromatography since these molecules can

be functionalized practically with any kind of chemical and even biological moieties. In the same way for these cases, adsorption capacity can be enhanced.

Furthermore, the method to produce these adsorbents is simple and cost effective, making it an attractive alternative to existing chromatographic adsorbent synthesis strategies. In general, it is believed that the novel dendronized adsorbents presented here can be considered for the separation of proteins and other high-value molecules by addressing some aspects like operation optimization and achieving a better control of dendron and ligand densities.

### Competing interests

The Tecnológico de Monterrey filed a patent on the synthesis of novel dendron-based adsorbents for HIC of proteins. MAMG, JAVG, MRP and JGV are listed in this application as inventors.

### Acknowledgments

The authors thank the FEMSA-Biotechnology Center at Tecnológico de Monterrey for the technological platform provided and the financial support of the Biotechnology and Synthetic Biology Focus Group (002EICIP01 and 0020DII001), the Chemistry and Nanotechnology Department (0020CDB088), and the National Council on Science and Technology of Mexico (CONACyT; project 242286). M.A.M.-G. also wishes to thank CONACyT for the fellowship No. 204152. S.Y. thanks the financial support of the EU-FP7-Marie Curie Action with the Grand Agreement PIRSES-GA 2010-269211.

### References

- [1] R. Freitag, *Chromatographic techniques in the downstream processing of proteins in biotechnology*, in: R. Pörtner (Ed.), *Animal Cell Biotechnology-Methods in Molecular Biology*, 2nd ed., Humana Press New Jersey, 2014, pp. 419–458.
- [2] J. González-Valdez, M. Rito-Palomares, J. Benavides, Advances and trends in the design, analysis, and characterization of polymer–protein conjugates for PEGylated bioprocesses, *Anal. Bioanal. Chem.* 403 (2012) 2225–2235, <http://dx.doi.org/10.1007/s00216-012-5845-6>.
- [3] C.C. Ibarra-Herrera, R. Reddy-Vennapusa, M. Rito-Palomares, M. Fernández-Lahore, Proteome wide evaluation of the separation ability of hydrophobic interaction chromatography by fluorescent dye binding analysis, *J. Mol. Recognit.* 26 (2013) 618–626, <http://dx.doi.org/10.1002/jmr.2302>.
- [4] K. Mayolo-Deloya, M.E. Lienqueo, B. Andrews, M. Rito-Palomares, J.A. Asenjo, Hydrophobic interaction chromatography for purification of monoPEGylated RNase A, *J. Chromatogr. A* 1242 (2012) 11–16, <http://dx.doi.org/10.1016/j.chroma.2012.03.079>.
- [5] M. Rito-Palomares, Practical application of aqueous two-phase partition to process development for the recovery of biological products, *J. Chromatogr. B* 807 (2004) 3–11, <http://dx.doi.org/10.1016/j.jchromb.2004.01.008>.
- [6] R. Sadavarte, M. Spearman, N. Okun, M. Butler, R. Ghosh, Purification of chimeric heavy chain monoclonal antibody EG2-hFc using hydrophobic interaction membrane chromatography: an alternative to protein-A affinity chromatography, *Biotechnol. Bioeng.* 111 (2014) 1139–1149, <http://dx.doi.org/10.1002/bit.25193>.
- [7] W. Marek, R. Muca, S. Woś, W. Piątkowski, D. Antos, Isolation of monoclonal antibody from a Chinese hamster ovary supernatant. II: dynamics of the integrated separation on ion exchange and hydrophobic interaction chromatography media, *J. Chromatogr. A* 1305 (2013) 64–75, <http://dx.doi.org/10.1016/j.chroma.2013.06.076>.
- [8] A.A. Shukla, J. Thömmes, Recent advances in large-scale production of monoclonal antibodies and related proteins, *Trends Biotechnol.* 28 (2010) 253–261, <http://dx.doi.org/10.1016/j.tibtech.2010.02.001>.
- [9] G. Glad, J.-L. Maloisel, N. Thevenin, Activated solid support and method, Patent No. US008217118B2 (2012).
- [10] S.C. March, I. Parikh, P. Cuatrecasas, A simplified method for cyanogen bromide activation of agarose for affinity chromatography, *Anal. Biochem.* 60 (1974) 149–152.
- [11] N. Feliu, M.V. Walter, M.I. Montañez, A. Kunzmann, A. Hult, A. Nyström, et al., Stability and biocompatibility of a library of polyester dendrimers in comparison to polyamidoamine dendrimers, *Biomaterials* 33 (2012) 1970–1981, <http://dx.doi.org/10.1016/j.biomaterials.2011.11.054>.
- [12] J. Khandare, M. Calderón, Dendritic polymers for smart drug delivery applications, *Nanoscale* 7 (2015) 3806–3807, <http://dx.doi.org/10.1039/c5nr90030a>.
- [13] A.-M. Caminade, C. Padié, R. Laurent, A. Maraval, J.-P. Majoral, Uses of dendrimers for DNA microarrays, *Sensors* 6 (2006) 901–914, <http://dx.doi.org/10.3390/s6080901>.
- [14] M. Jaćkowska, S. Bocian, B. Buszewski, Dendrimer modified silica gel for anion exchange chromatography: synthesis, characterization and application, *Analyst* 137 (2012) 4610–4617, <http://dx.doi.org/10.1039/c2an35312a>.
- [15] C.-C. Chu, N. Ueno, T. Imae, Solid-phase synthesis of amphiphilic dendron-surface-modified silica particles and their application toward water purification, *Chem. Mater.* 20 (2008) 2669–2676, <http://dx.doi.org/10.1021/cm702401s>.
- [16] M.M. Bradford, A rapid and sensitive method for the quantitation of microgram quantities of protein utilizing the principle of protein-dye binding, *Anal. Biochem.* 72 (1976) 248–254, [http://dx.doi.org/10.1016/0003-2697\(76\)90527-3](http://dx.doi.org/10.1016/0003-2697(76)90527-3).
- [17] U.K. Laemmli, Cleavage of structural proteins during the assembly of the head of bacteriophage T4, *Nature* 227 (1970) 680–685, <http://dx.doi.org/10.1038/227680a0>.
- [18] N. Dyballa, S. Metzger, Fast and sensitive colloidal coomassie G-250 staining for proteins in polyacrylamide gels, *J. Vis. Exp.* 30 (2009) 1431, <http://dx.doi.org/10.3791/1431>.
- [19] K. Wrzosek, M. Gramblička, M. Polakovič, Influence of ligand density on antibody binding capacity of cation-exchange adsorbents, *J. Chromatogr. A* 1216 (2009) 5039–5044, <http://dx.doi.org/10.1016/j.chroma.2009.04.073>.
- [20] A. Susanto, T. Herrmann, E. von Lieres, J. Hubbuch, Investigation of pore diffusion hindrance of monoclonal antibody in hydrophobic interaction chromatography using confocal laser scanning microscopy, *J. Chromatogr. A* 1149 (2007) 178–188, <http://dx.doi.org/10.1016/j.chroma.2007.03.002>.
- [21] A. Kosior, M. Antošová, R. Faber, L. Villain, M. Polakovič, Single-component adsorption of proteins on a cellulose membrane with the phenyl ligand for hydrophobic interaction chromatography, *J. Membr. Sci.* 442 (2013) 216–224, <http://dx.doi.org/10.1016/j.memsci.2013.04.013>.
- [22] E. Müller, Properties and characterization of high capacity resins for biochromatography, *Chem. Eng. Technol.* 28 (2005) 1295–1305, <http://dx.doi.org/10.1002/ceat.200500161>.
- [23] N. Shoji, A. Matsui, M. Omote, N. Kuriyama, B. Blödorn, D. Kune, et al., Facing the challenges in bio-pharmaceutical production: developments in ion exchange media to bring down cost of goods, *Chromatogr. Today* (2009) 38–40 [www.chromatographytoday.com/article\\_read/571/](http://www.chromatographytoday.com/article_read/571/).